Optimization of kinetostatic performances and compactness of an in vivo serial robot for minimally invasive surgery

Christophe Drouin, Sylvain Miossec, Carl A. Nelson, Gérard Poisson

Optimization of kinetostatic performances and compactness of an *in vivo* serial robot for minimally invasive surgery

C. Drouin[a], S. Miossec[a], C.A. Nelson[b], G. Poisson[a]

a. *University of Orleans, PRISME Laboratory, Bourges, Centre, FRANCE*
b. *University of Nebraska-Lincoln, Mechanical and Materials Engineering, Lincoln, NE, USA*

Résumé :

Dans cet article, nous optimisons les dimensions des corps d'un robot de chirurgie mini-invasive muni de deux bras sériels pour améliorer ses performances cinétostatiques (force, vitesse) ainsi que sa compacité, sous contraintes d'espace atteignable. Une courbe de Pareto est tracée pour fournir au concepteur toutes les solutions optimales possibles entre les vitesses, les forces transmises ainsi que la compacité.

Abstract :

In this paper, we optimize the link dimensions of a robot with two serial arms for minimally-invasive surgery, to improve its kinetostatic performance (force, velocity) and its compactness, under the constraint of reachable space. A Pareto curve is plotted to provide the designer all the optimum possible solutions between transmissible velocity, forces, and compactness.

Mots clefs : medical robots ; optimal design ; multiobjective optimization ; dimensional synthesis

1 Introduction

The medical application of minimally invasive surgery (MIS) is a different technique compared to open surgery, which consists of operating on the patient through holes to reduce operative trauma stress. Laparoendoscopic single-site surgery (LESS) is another technique based on MIS : the surgeon passes his instruments through a single hole instead of multiple ones. The complexity of the required movements in these techniques highlights the utility of robotic systems to help the surgeon. For LESS purposes, the *in vivo* robots present a challenging design to simultaneously avoid collisions, seek for the best compactness and get the best end-effector velocity and force (kinetostatic performance).
At the University of Nebraska-Lincoln, several robots have been developed [2, 4, 8, 10]. Workspace, kinetostatic performance and simplicity of insertion were the major points of development and evolution of these robots. Many compromises in the design need to be made, difficult to solve with a CAD approach. In this paper, we present the dimensional synthesis of such an *in vivo* robot, mathematically formulated, to improve simultaneously its compactness and its kinetostatic performance, while taking into account workspace constraints. Section 2 will describe the robot (kinematic model, Jacobian and singularities), Section 3 will present the dimensional optimization to improve its global performances.

2 Robot overview

2.1 Robot structure

The robot has a 2R-R-R architecture (Figure 1) and is a two-armed serial robot. Its kinematic architecture and Denavit-Hartenberg parameters [6] are presented in Figure 2 and Table 1, with $j = 1..2$, corresponding to the right and left arm.

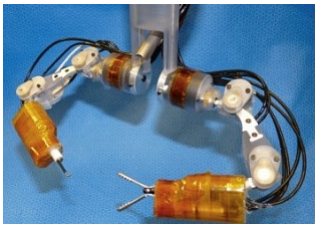

Figure 1 – Robot structure

Joint	1	2	3	4
α_{i-1j}	$(-1)^{j+1}\frac{\pi}{2}$	$(-1)^{j+1}\frac{-\pi}{2}$	0	$\frac{-\pi}{2}$
a_{i-1j}	0	0	a_{2j}	0
θ_{ij}	θ_{1j}	θ_{2j}	θ_{3j}	θ_{4j}
r_{ij}	r_{1j}	0	0	r_{4j}
θ (fig. 2)	$\delta\theta_{11}$	0	$\frac{-\pi}{2}+\delta\theta_{31}$	$\frac{-\pi}{2}$
ω (rad/s)	0.97	1.11	1.11	/
T (Nmm)	1220.61	264.17	264.17	/

Table 1 – Denavit-Hartenberg parameters

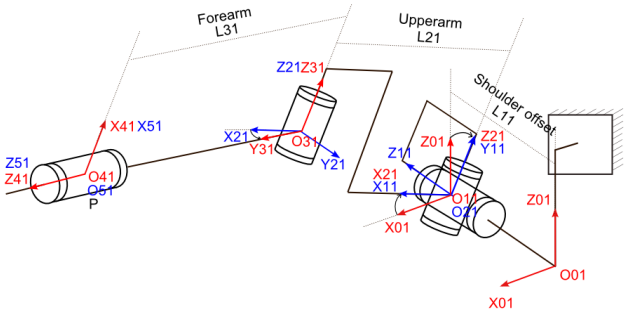

Figure 2 – Kinematic architecture (right arm)

We have $r_{1j} = L_{1j}$, $a_{2j} = L_{2j}$ and $r_{4j} = L_{3j}$. L_{1j} defines the shoulder offset equal to 17.5 mm while L_{2j} and L_{3j} are the parameters to optimize.

2.2 Direct and inverse model

The direct model is the expression of the end effector position in operational space, function of joint motions, as written below (the 4^th actuator as no influence on the robot position) :

$$\begin{pmatrix} PX_j \\ PY_j \\ PZ_j \end{pmatrix} = f(\begin{pmatrix} \theta_{1j} \\ \theta_{2j} \\ \theta_{3j} \end{pmatrix}) \tag{1}$$

For the right arm, we will have :

$$\begin{pmatrix} PX_1 \\ PY_1 \\ PZ_1 \end{pmatrix} = \begin{pmatrix} c_{\theta_{11}}(c_{\theta_{21}}(L_{21} - L_{31}s_{\theta_{31}}) - L_{31}s_{\theta_{21}}c_{\theta_{31}}) \\ s_{\theta_{21}}(L_{21} - L_{31}s_{\theta_{31}}) + L_{31}c_{\theta_{21}}c_{\theta_{31}} - L_{11} \\ s_{\theta_{11}}(c_{\theta_{21}}(L_{21} - L_{31}s_{\theta_{31}}) - L_{31}s_{\theta_{21}}c_{\theta_{31}}) \end{pmatrix} \tag{2}$$

and the equations of the inverse model are :

$$\begin{pmatrix} \theta_{11} \\ \theta_{21} \\ \theta_{31} \end{pmatrix} = \begin{pmatrix} atan2(PZ_1, PX_1) \\ atan2(\alpha(L_{11} - \gamma\ L_{21}) - \beta\ \lambda\ L_{21}, \alpha\ L_{21}\ \lambda + \beta(L_{11} - L_{21}\ \gamma)) \\ atan2((L_{21}^2 - \alpha^2 - \beta^2 + L_{11}^2)/(2L_{11}), \pm\sqrt{\alpha^2 + \beta^2 - L_{11}^2 + 2\gamma\ L_{11}L_{21} - \gamma^2 L_{21}^2}) \end{pmatrix} \tag{3}$$

with :

$$\alpha = PZ_1 - L_{11},\ \beta = -PZ_1 s_{\theta_{11}} - PX_1 c_{\theta_{11}},\ \gamma = s_{\theta_{31}},\ \lambda = c_{\theta_{31}} \tag{4}$$

The study of the inverse model shows there is no solution in two different cases, corresponding to the unreachable positions of the robot as described in the following section.

2.3 Jacobian and singularities

The direct instantaneous kinematic model gives the relation between the joint angular velocities and the end-effector velocities :

$$\dot{X}_j = J_j\dot{Q}_j,\ Q_j = [\theta_{1j}\ \theta_{2j}\ \theta_{3j}]^T \tag{5}$$

With J_1 detailed as follow :

$$J_1 = \begin{pmatrix} L_{31}s_{\theta_{11}}(s_{\theta_{31}+\theta_{21}} - L_{21}c_{\theta_{21}}) & -L_{31}c_{\theta_{11}}(c_{\theta_{31}-\theta_{21}} - L_{21}s_{\theta_{21}}) & -L_{31}c_{\theta_{11}}c_{\theta_{21}+\theta_{31}} \\ 0 & -L_{31}(c_{\theta_{21}+\theta_{31}} + L_{21}c_{\theta_{21}}) & -L_{31}c_{\theta_{21}+\theta_{31}} \\ -L_{31}c_{\theta_{11}}(c_{\theta_{21}+\theta_{31}} + L_{21}c_{\theta_{21}}) & -L_{31}s_{\theta_{11}}(c_{\theta_{31}-\theta_{21}} + L_{21}s_{\theta_{21}}) & -L_{31}s_{\theta_{11}}c_{\theta_{21}+\theta_{31}} \end{pmatrix} \quad (6)$$

The study of these three vectors indicates three cases of singularities. The first one appears when the forearm and upper arm are aligned or bent over backwards ; this indicates the exterior and interior boundaries of the workspace, giving a hollow sphere (Figure 3). The second one is physically infeasible : it appears when $\theta_{21} = 0$ with $L_{21} = 0$. The last case indicates an unreachable area, represented by a line, in this sphere, as indicated in Figure 3, in sandy-brown.
Other voids depend on motion limits of the joints and on collisions of the robot mechanical parts, which are not considered in this paper.

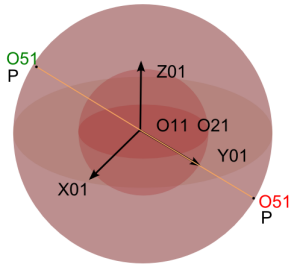

Figure 3 – Robot workspace

3 Optimization

3.1 Data

The shape formed by the desired reachable tool-positions is approximated by an ellipsoid whose semi-major and semi-minor axes are determined based on the minimal and maximal bounds of some data presented in [8]. These data are based on two operations (open cholecystectomy and colectomy), performed on a porcine model. The two data sets give two ellipsoids for the two arms.

3.2 Constraints

Considering the fact the robot-arm workspace is a hollow sphere, the two ellipsoids must be inside the reachable positions of their spheres. Assuming that $L_{3j} < L_{2j}$, we must have $L_{2j} - L_{3j} < min(D_{S_j})$ and $L_{2j} + L_{3j} > max(D_{S_j})$, with D_{Sj} the set of distances from O_{1j} to a desirable position M_{nj}. These two workspace constraints will be written as $C_{W_{1j}}$ and $C_{W_{2j}}$.
The second type of constraint concerns the collisions that may occur between the two arms during an operation : they can be avoided if $\theta_{11} \in [-180^\circ; 0^\circ]$ and $\theta_{12} \in [0^\circ; 180^\circ]$, meaning that two different solutions to the inverse model of the two arms must be considered.

3.3 Performance criteria

Based on Briot's work [1], two kinetostatic performance criteria are optimized i.e. $P_{Velocity} = \min_{S_j}(k^{min}_{Vij})$ and $P_{Force} = \min_{S_j}(k^{min}_{Fij})$. They are defined as the lowest values of velocity and forces in the workspace S_j, where S_j is the set of the tool-tip positions to reach, $S_j = \{M_{1j}; M_{2j}...; M_{nj}\}$. $j = 1$ for left-arm and $j = 2$ right-arm since the two sets contain different points. The k^{min}_{Vij} factor represents the smallest velocity in a direction at the end-effector, for a given point M_{ij}. It will be zero when a serial singularity is met at this point. $k^{min}_{Vij} = min_j(k^m_{ghl}) = \sqrt{J^T_{2j}J_{2j} - (J^T_{2j}J_{1j})(J^T_{1j}J_{1j})^{-1}(J^T_{1j}J_{2j})}$, where $J_{2j} = [I_{gj}\ I_{hj}]$, $J_{1j} = (-1)^m I_{lj}$, for $g, h, l = 1, 2, 3$, $g \neq h \neq l$, $m = 1$ or 2, with $[I_{1j}\ I_{2j}\ I_{3j}] = J_j\ diag(\dot{\theta}_{kjmax})$. $\dot{\theta}_{kjmax}$ represents the maximal velocity of the k^{th} actuator of the j^{th} arm. We also have $k^{max}_{Vj} = max_l(\|J_j(q)e_l\|)$, for l=1 to 4,

with $e_1 = [1; -1; 1]^T$ $e_2 = [1; 1; 1]^T$ $e_3 = [1; 1; -1]^T$ $e_4 = [1; -1; -1]^T$.
The evaluation of minimal forces $k^{min}_{Fij\ S_j}$ is done with the same previous definition by replacing $J_j\ diag(\dot{\theta}_{kjmax})$ by $J_j^{-T}\ diag(T_{kjmax})$, where T_{kjmax} represents the maximal torque of the k^{th} actuator of the j^{th} arm. k^{min}_{Fij} represents the smallest force in a direction at the end-effector. This factor can also be calculated through a statical equilibrium.
Compared to some indices like the dexterity [3] or the manipulability [11], those presented [1] are more suitable when the actuators characteristics are known. Indeed, if performance is related to precision, isotropy or the identification of singularities, dexterity or manipulability are well adapted but they do not take into account the heterogeneity of the actuators since they consider the norm of the input velocities equal to one, which is not the physical reality [7]. Dexterity and manipulability are criteria used as a first robot predimensioning when its actuators characteristics are not known. The advantages of using Briot'criteria is sum up as follow :

– The heterogeneity of actuators is taken into account
– If dexterity or manipulability are used, an implicit compromise is done between optimal velocities and forces ; using Briot'criteria enables to consider minimal velocities and forces independentely.
– The input velocities are not some ellipsoïds in force or velocity but some boxes which represent the physical reality
– The dexterity or the manipulability gives values between $[0; 1]$ and $[0; \infty]$, while k^{min}_{Vij} and k^{min}_{Fij} are more easily interpretable values for the design objectives.

The last criterion to optimize in the problem is the compactness ; this criterion has been simply defined as the sum of lengths L_{2j} and L_{3j}, as follows : $P_{Compactness_j} = L_{2j} + L_{3j}$

3.4 The objective function

A gradient-based method was used to find the optimal parameters satisfying the constraints and giving the optimal solutions between compactness and kinetostatic performances. The problem was formulated as follows : $min\ f(X)_j = \beta[(1-\alpha)(P_{Compactness_j}) + \alpha N(P_{Velocity_j})] + (1-\beta)(P_{Force_j}),\ subject\ to$ $C_{Wkj}(X) > 0,\ k = 1...2$. X represents the vector of design variables, defined as follow : $X = (L_{2j}; L_{3j})$ with N a normalization coefficient, α and β two weighting coefficients between the three criteria, $\alpha, \beta \in [0; 1]$ to compute the Pareto curve as explained below.

3.5 Results and Comparison with another architecture

Results of optimization are presented in Figures 4, 5 and 6 for the left arm : results and interpretations of the right one are similar. ($P_{Velocity}$ is in mm/s and P_{Force} is in N). Each point is an optimal solution (L_{2j}, L_{3j}), obtained by varying α and β. One can see the compact solution figure 6 in XZ plan, and the same solution in XY plan figure 5.

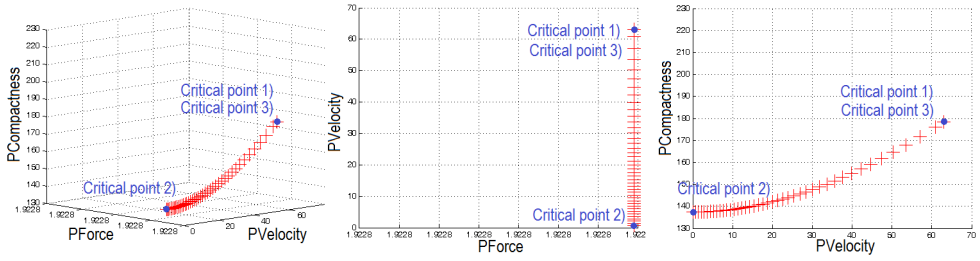

Figure 4 – Pareto curves for the left arm ($P_{Velocity}$ in mm/s, P_{Force} in N and $P_{Compactness}$ in mm).

We define the three critical points as 1) the maximum of $P_{Compactness}$, 2) the minimum of $P_{Velocity}$ and 3) the compromise between $P_{Velocity}$ and $P_{Compactness}$. For the last one, we define the compromise between compactness and velocity as the opposite relative variations [9] ; we would have $dP_{Compactness}/P_{Compactness} = -P_{Velocity}/P_{Velocity}$; with this definition, for a small variation along the Pareto front that will improve one criterion by 1%, it will degrade the other criterion by 1%.

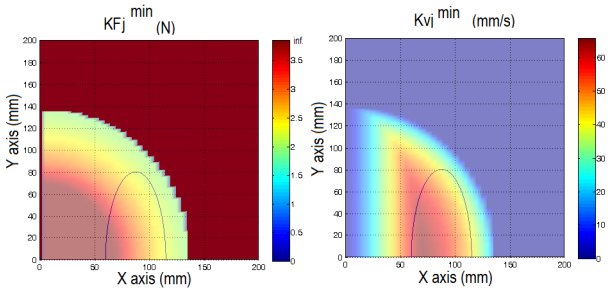

Figure 5 – Evolution of k_{Vj}^{min} (in mm/s) and k_{Fj}^{min} (in N) for point 2) in XY plan (left arm)

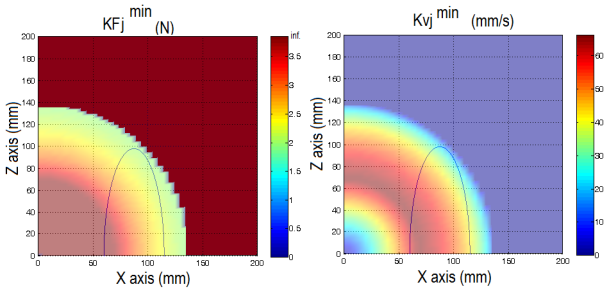

Figure 6 – Evolution of k_{Vj}^{min} (in mm/s) and k_{Fj}^{min} (in N) for point 2) in ZX plan (left arm)

Results of optimization for the left and right arm are indicated below (L_{2j} and L_{3j} are in mm, $P_{Compactness}$ is in mm, $P_{Velocity}$ in mm/s and P_{Force} in N).
$(L_{2j}; L_{3j}) = (68.69; 68.69), P_{Compactness} = 137.38, P_{Velocity} = 0.009, P_{Force} = 1.92$ (point 2)).
$(L_{2j}; L_{3j}) = (89.13; 89.13), P_{Compactness} = 178.27, P_{Velocity} = 63.05, P_{Force} = 1.92$ (point 1) and 3)).
Results of optimization for the right arm :
$(L_{2j}; L_{3j}) = (117.5; 62.5), P_{Compactness} = 180, P_{Velocity} = 0.009, P_{Force} = 1.46$ (point 2)).
$(L_{2j}; L_{3j}) = (104.15; 104.15), P_{Compactness} = 208.31, P_{Velocity} = 58.20, P_{Force} = 1.46$ (point 1) and 3)).

Firstly, the results show point 3) is mingled with point 1). It means that from a mechanical point of view, it is unprofitable to improve the compactness since it highly reduces the velocity.
Secondly, we see P_{Force} has the same value 1.92N on the Pareto, i.e. for any couple $(L_{21}; L_{31})$. To explain that, we recall P_{Force} represents the lowest value of force for a couple $(L_{21}; L_{31})$, in the workspace S_j. This value is the ratio between the maximal torque $T_{21} = 264.17\ Nmm$ of the second joint and the distance from O_{11} to the farther point of the workspace $d_{max} = 137\ mm$. It can be seen as the lever arm of the 2nd joint to the farther point of the workspace.
Thirdly, the results show it is useless to increase the link lengths to improve $P_{Velocity}$: it reaches a limit at 63.05 mm/s. This value corresponds to the product between the maximal velocity $V_{11\ max} = 0.97\ rad/s$ of the 1st joint by the distance from O_{11} to the closest point of the workspace in ZX plane ($d_{min_{zx}} = 65\ mm$). This can be seen as the lever arm of the 1st joint to the closest point of the workspace. It indicates that increasing the lengths is useless, but to respect $C_{W_{1j}}$ (closest-point constraint).

All these results indicates the minimal force depends on the 2nd joint while the minimal velocity depends on the 1st one. It can be seen as guidelines for future enhancements in the choice of actuator and elements of transmission.

Such a dimensional synthesis was previously performed for the same purposes, but with another architecture [5]. The two first joint were interchanged, giving another workspace ; in particular, two spherical voids were contained in the hollow sphere, giving more constrained results. This interchangement was done according to some integration constraint, due to the medical operation process. The actuators characteristics were also different, giving other kinetostatic performances. Results of its optimization for the left and right arm are indicated below (L_{2j} and L_{3j} are in mm, $P_{Compactness}$ is in mm, $P_{Velocity}$ in mm/s and P_{Force} in N).
Results of optimization for the left arm :
$(L_{2j}; L_{3j}) = (101.29; 36.10), P_{Compactness} = 137.39, P_{Velocity} = 0.64, P_{Force} = 6.80$ (point 2))
$(L_{2j}; L_{3j}) = (111.12; 63.51), P_{Compactness} = 174.64, P_{Velocity} = 85.25, P_{Force} = 3.87$ (point 1) and 3)).
Results of optimization for the right arm :
$(L_{2j}; L_{3j}) = (120.00; 60.00), P_{Compactness} = 180.00, P_{Velocity} = 0.46, P_{Force} = 4.09$ (point 2))
$(L_{2j}; L_{3j}) = (123.14; 71.82), P_{Compactness} = 194.94, P_{Velocity} = 60.54, P_{Force} = 3.42$ (point 1) and 3)).

The results has shown P_{Force} had not the same value, compared to our robot in the Pareto. Moreover, for any couple $(L_{21}; L_{31})$, P_{Force} was constant in the workspace S_j : the 3rd joint was the limitation of P_{Force} for any configuration in S_j instead of the 2nd one for our robot.

It is interesting to note the kinetostatic performances are better for this robot than the one presented in this paper, though we would have expected the opposite. This is due to technological choice (less powerful motor) and it indicates the kinetostatic performances of our robot could be largely better, with an appropriate choice of actuators and gear ratios.
Futhermore, our robot workspace is less problematic for an optimum design compared to the other one : the sequence of the 1st and 2nd link is different and creates some spherical voids in the workspace, while we only have lines here. The topology has a major influence on the robot kinetostatic performances.

All these results of optimization indicates one major thing : it is necessary to couple the dimensional synthesis with the choice and integration of actuators. These two phases of design cannot be performed independently or sequentially.

4 Conclusion

In this paper, the dimensional synthesis of a two-arm robot with 2R-R-R architecture has been presented, for LESS surgery. The link dimensions have been optimized to give the designer the solutions balancing the lowest velocity, force and the better compactness, under constraints of workspace. It has been performed taking into account the actuator characteristics. The results show the under-dimensioning of some actuators ; in particular, it would be interesting to re-dimension the actuators of the 2nd joint and the 1st one to improve the kinetostatic performances.
A brief comparison with another similar 2R-R-R architecture highlights the need to couple simultaneously the dimensional synthesis with the choice of actuators. Our future work will therefore concern the re-dimensioning of the actuators for this robot. Ideally, the dimensional synthesis could be coupled with the integration of actuators, which could be done under workspace constraint, more realistic collisions constraints, but also some insertion and integration constraints.

Références

[1] Briot S. Pashkevich A. and Chablat D. Optimal technology-oriented design of parallel robots for high-speed machining applications. *International Conference on Robotics and Automation*, 2010.

[2] Pourghodrat A. Nelson C. A. and Midday J. Pneumatic miniature robot for laparoendoscopic single incision surgery. *International Design Engineering Technical Conference*, 2011.

[3] Gosselin C. and Angeles J. The optimum design of a spherical three-degree-of-freedom parallel manipulator. *Journal of Mechanisms, Transmissions, and Automation in Design*, 111, No 2 :202–207, 1989.

[4] Piccigallo M. Scarfogliero U. Quaglia C. and Petroni G. Design of a novel bimanual robotic system for single-port laparoscopy. *Transactions on Mechatronics*, 2010.

[5] Drouin C. Pourghodrat A. Miossec S. Poisson G. and Nelson C. A. Dimensional optimization of a two-arm serial robot for single-site surgery operations. *International Design Engineering Technical Conference*, 2013.

[6] Denavit J. and Hartenberg R. A kinematic notation for lower-pair mechanisms based on matrices. *Journal of Applied Mechanics*, 1955.

[7] Merlet J.P. Jacobian, manipulability, condition number, and accuracy of parallel robots. *Journal of Mechanical Design*, 2006.

[8] Wortman T. D. Strabala K. W. Lehman A. C. Farritor S. M. and Oleynikov D. Laparoendoscopic single-site surgery using a multi-functional miniature in vivo robot. *International Journal of Medical Robotics and Computer Assisted Surgery*, 2011.

[9] S. Miossec and L. Nouaille. Structural link optimization of an echography robot. *IFToMM*, 2011.

[10] Lehman A.C. Wood N.A. Farritor S. Goede M.R. and Oleynikov D. Dexterous miniature robot for adavanced minimally invasive surgery. *Surgical Endoscopy*, 2011.

[11] Yoshikawa T. Manipulability of robotic mechanisms. *Intenational Journal of Robotics Research*, 1985.